https://doi.org/10.48048/tis.2022.6270

Synthesis and Characterization of Zeolite NaY and its Glyphosate Adsorption Capacity with Varying Iron Content

Onsulang Sophiphun[1,*], Worapong Bua-ngern[2], Sontichai Chanprame[3,4] and Chanakan Laksana[1]

[1]Department of Agricultural Innovation, Faculty of Agricultural Technology, Burapha University Sakaeo campus, Sakaeo 27160, Thailand
[2]Department of Applied Chemistry, Faculty of Sciences and Liberal Arts, Rajamangala University of Technology Isan, Nakhon Ratchasima 30000, Thailand
[3]Center for Agricultural Biotechnology, Kasetsart University and The Center of Excellence on Agricultural Biotechnology (AG-BIO/PERDO)/CHE, Bangkok 10900, Thailand
[4]Department of Agronomy, Faculty of Agriculture at Kamphaeng Saen, Kasetsart University, Nakhon Pathom 73140, Thailand

([*]Corresponding author's e-mail: onsulang@buu.ac.th)

Received: 20 October 2022, Revised: 27 October 2022, Accepted: 31 October 2022, Published: 1 November 2022

Abstract

In this study, Fe loaded zeolite NaY with varying iron contents was prepared and used as glyphosate adsorbents. A hydrothermal method was used to synthesize the zeolite NaY from bagasse ash derived silica (Si-BA). Various Fe contents (1.75 - 7.66 %w/w) were impregnated onto the zeolite. Several techniques were used to examine the physicochemical properties of adsorbents, including X-ray diffraction (XRD), energy dispersive X-ray fluorescence (ED-XRF), N_2 adsorption-desorption, field emission scanning electron microscopy (FE-SEM), pH drift method, and zeta potential. In a batch adsorption process with an initial glyphosate concentration of 50 mg/L at pH 4, the effect of contact time was investigated. The pseudo second order kinetic model fitted the experimental data well, indicating that chemisorption controlled the rate determining step for all adsorbents. The Fe loaded zeolite NaY outperformed the bare zeolite NaY in terms of adsorption capacity. The rate constant (K_2) and adsorption capacity at equilibrium time (qe) increased when the adsorbents were used in the following order: 1.75 < 5.11 < 7.66 %Fe/NaY. Furthermore, the intra-particle diffusion model was fitted to the experimental data, with a correlation coefficient R^2 greater than 0.95. The findings demonstrated that both internal and external diffusion contributed to the rate-determining step. The Langmuir and Freundlich adsorption isotherm models were used to depict the glyphosate adsorption mechanism by the adsorbents. The Freundlich adsorption isotherm best explained all of the data. Glyphosate was thus multilayer adsorbed on the heterogeneous surfaced adsorbents. The adsorption of glyphosate increased as the Fe content, which is primarily due to complexation between Fe and the glyphosate molecule.

Keywords: Glyphosate, Adsorption, Zeolite NaY, Fe, Bagasse ash

Introduction

Thailand is an agricultural country that exports rice, cassava, rubber, and fruits to the world market [1]. One of the most commonly used herbicides in crop production is glyphosate, N-(phosphonomethyl glycine), which has been imported in the greatest quantity over the last decade and is widely used as a non-selective weed killer [2]. After spraying glyphosate to the target plants, it inhibits the biosynthesis of aromatic amino acids from shikimic acid pathway resulted in the dead plants within 10 - 20 days [3]. Long-term glyphosate use results in glyphosate-resistant plants, which increases the consumption volume. As a result, glyphosate may contaminate soil and surface water in many areas of Thailand [4,5]. In 2015, the International Agency for Research on Cancer classifies glyphosate as probably carcinogenic to humans (Group 2A) [6]. Many attempts have been undertaken to study the adsorption of glyphosate from aqueous solutions, as evidenced by a number of publications. Glyphosate molecules contain nitrogen (N) and oxygen (O), which act as Lewis bases and can coordinate with metals (M+) to form a stable complex. The most stable complexes are in the following order Fe^{3+}-glyphosate > Al^{3+}-glyphosate > Cu^{2+}-glyphosate > Zn^{2+}-

glyphosate > Fe^{2+}-glyphosate > Mn^{2+}-glyphosate > Ca^{2+}-glyphosate > Mg^{2+}-glyphosate [7,8]. From the work of Barja *et al.* (1998), they studied the ATR-FTIR spectra in aqueous solution of the 1:1 Fe^{3+}/glyphosate complex at pH of 4. The glyphosate showed an evidence of coordinating the metal through the phosphonic group [9]. Sheals *et al.* (2018) also studied the adsorption of glyphosate on the surface of goethite (α-FOOH) and monitored by ATR-FTIR techniques [10]. They found that the phosphonic group of glyphosates bound to the goethite surface forming monodentate inner-sphere complex. The glyphosate could interact with the supported metal faster than the soluble metal in a liquid media [11]. To increase the adsorption of glyphosate, Fe was dispersed on various types of porous support. For instance, Fe loaded on modified carbons [12,13], montmorillonite [14], resin [15], metal oxide [11] and metal organic framework [16].

Zeolites are one of the promising adsorbents for pesticide removal. They are well-defined porous materials with a high specific surface area and good thermal stability, able to reuse for many cycles. Milijević-Rakić *et al.* (2013) studied the adsorption of glyphosate by zeolite ZSM-5. The maximum adsorption capacity of ZSM-5 was 14.9 mg/g when the initial glyphosate concentration of 4,000 mg/L at the sorption equilibrium of 2 h [17]. For Janićijević *et al.* (2021), the zeolite BEA and Ag/BEA were tested for glyphosate adsorption. They found that the maximum adsorption capacities were 114 and 102 mg/g from Krishnamurti isotherm model for BEA and Ag-BEA, respectively [18]. Moreover, the zeolite 4A and Cu/zeolite 4A were employed for the adsorption. The Cu/zeolite 4A exhibited a higher glyphosate adsorption capacity than the zeolite 4A. The maximum adsorption capacity of Cu/zeolite 4A was 112.7 mg/g using the fitted Langmuir model [19]. Zeolite's silanol group and Brønsted acid site formed hydrogen bonds with glyphosate [18]. Meanwhile, the loaded metal acted as a Lewis acid site, allowing it to interact with the glyphosate phosphonic group via chemisorption. Considerably, the molecular size of glyphosate was 0.30 - 0.53×0.77×0.45 nm^3 [20]. Therefore, the zeolite with small pore sizes as zeolites ZSM-5, BEA, and 4A might retard the adsorption of glyphosate inside the zeolite pore. Yang *et al.* (2019) studied the removal of phenol through the Fenton-type reaction. The Fe_2O_3 was dispersed over the zeolite ZSM-5, MOR and NaY by impregnation method. They discovered that the Fe_2O_3 was well dispersed on the zeolite NaY and provided superior phenol degradation efficiency over the other zeolites. Because the zeolite NaY has a large surface area and a 3-dimensional 12-MR channel system with a pore diameter of 0.74 nm, it is suitable for use in adsorption applications. Furthermore, the zeolite with low Si/Al ratios resulted in its hydrophilic properties which aided in the deep infiltration of the impregnated Fe, which served as an active site for the reaction [21]. To the best of our knowledge, there have been no reports of glyphosate adsorption using zeolite NaY.

In this study here, the Fe loaded zeolite NaY was used as adsorbent for adsorption of glyphosate in a batch process. The zeolite NaY was first synthesized from bagasse ash silica through a hydrothermal method and then being loaded with Fe by impregnation method. We compared the effects of different Fe loadings on glyphosate adsorption. To understand the kinetic behavior and adsorption mechanism, the pseudo-first order model (PFO), pseudo-second order model (PSO), Elovich model (ELV), and intra-particle diffusion model (IPD) were applied to the kinetic adsorptions. Finally, the adsorption isotherms were studied by Langmuir and Freundlich adsorption isotherm models to get more information about the interaction between the prepared adsorbents and glyphosate molecules.

Materials and methods

Materials

Bagasse ash obtained from the Eastern sugar & cane Co., Ltd., Sakaeo, Thailand. Silica which a raw material for a synthesis of zeolite NaY was extracted from the bagasse ash. Chemicals used for the silica extraction and the zeolite synthesis were following NaOH (99 wt%, Merck), concentrated H_2SO_4 (98 wt%, ANaPURE®) and $NaAlO_2$ (55 - 56 wt%, Riedel-de Haën). Then $FeSO_4.7H_2O$ (99.5 - 102.0 wt%, Merck) was loaded onto the zeolite NaY by an impregnation method. For the glyphosate adsorption study, chemicals used were following glyphosate ($C_3H_8NO_5P$, 99.5 wt%, SIGMA-ALDRICH), ninhydrin ($C_9H_4O_3.H_2O$, 99 wt%, Ajax Finechem), sodium molybdate ($Na_2MoO_4.2H_2O$, 99.5 wt%, Ajax Finechem).

Methods

Extraction silica from bagasse ash

Silica was extracted from the obtained bagasse ash by a dissolution-precipitation method adapted from the work of Chindaprasirt and Rattanasak (2020) [22]. For the dissolution step, the bagasse ash was firstly rinsed with DI water to remove dust and dried at 100 °C overnight. The mixture of bagasse ash: 2 M NaOH solution of 12.0 g:100 mL was well stirred at 400 rpm for 36 h. After that the solution was separated

by a vacuum filtration. For the precipitation step, the obtained solution was stirred and heated to 90 - 95 °C before drop wised 3 M H_2SO_4 to the solution until the pH was approximately 11. The cloudy slurry occurred indicating the silica precipitation. It was left at this condition for 3 h before continuously added 3 M H_2SO_4 until the pH of 7. Lastly, the silica was centrifuged, washed and dried at 120 °C for 24 h. The obtained solid was silica from bagasse ash.

Preparation of zeolite NaY and iron loaded zeolite NaY

Zeolite NaY was synthesized through a hydrothermal method adapted from the work of Rintramee *et al.* [23]. Firstly, the seed gel was prepared by dissolving 6.67 g NaOH: 2.09 g $NaAlO_2$: 6.52 g Si-BA in 20 mL DI H_2O. The gel was further aged at room temperature for 24 h. Then the feedstock gel was prepared by dissolving 16.39 g NaOH: 13.09 g $NaAlO_2$: 40.88 g Si-BA in 131 mL DI H_2O. The 16.50 g seed gel was slowly added into the prepared feedstock gel and stirred until getting a clear gel. After that the overall gel was transfer into a polypropylene bottle, which was tightly capped, and left for a crystallization at 100 °C 24 h in a hot air oven. The sample was then cooled to a room temperature, centrifuged washed and dried at 120 °C for 24 h. Finally, the obtained product was zeolite NaY. It was being impregnated with Fe by varying the metal contents (1.75 - 7.50 %w/w). $FeSO_4.7H_2O$ was used as a substance for the Fe loading. It was dissolved in DI H_2O and impregnated onto the zeolite NaY with the ratio of 2 mL/g. The obtained solid was dried at room temperature overnight and further dried at 120 °C for 12 h. Then it was calcined at 450 °C for 3 h. The obtained solids are denoted as x% Fe/NaY, where x is the mass percentage of Fe derived from ED-XRF techniques.

Characterizations

Sample structure was identified by XRD (Bruker AXS D5005) with Cu Kα radiation and nickel filtered at 40 mA and 40 kV in the range 2θ of 5 - 50 °. Elemental content was analyzed by ED-XRF (PANalytical Epsilon^{3x}) using Rh as anode material at 1.0 mA and 50 kV with a high resolution Si drift detector. N_2 adsorption-desorption isotherms were measured by BELLSORP mini II, Bell model. The samples were outgassed at 300 °C for 24 h until the pressure reached 10^{-2} MPa before an analysis. Total surface area (S_{BET}) and total pore volume (V_p) of materials were analyzed by using Brunauer-Emmett-Teller (BET) and Barrett-Joiner-Halenda (BJH) methods, respectively. The pH_{PZC} of samples was determined by a pH drift method. A series of 0.01 M NaCl aqueous solution was prepared with the $pH_{initial}$ of 2, 4, 6, 7, 8 and 10 by using 0.1 M NaOH and 0.1 M HCl. The precious pH values were recorded by pH meter (METTLER TOLEDO). Then the sample was added to a series of the adjusted pH solution and stirred for 24 h at a speed of 300 rpm. The solution's pH_{final} was measured in which the value equivalents to the pHinitial is pHpzc. Zeta potential (ζ) of samples was determined by zetasizer Nano ZS90 (Malvern PANalytical) and using the measurement technique of Lazer Doppler electrophoresis. The sample (0.2 g) was dispersed in DI H_2O water (10 mL) adjusted pH of 4 by 0.1 M NaOH and 0.1 M HCl. The colloidal solutions were taken to estimate the particle surface charge. The morphology of samples was studied by FE-SEM (Zeiss AURIGA) with the accelerator voltage of 5 kV. The sample was gently dispersed onto the carbon tape mounted to the copper stub. Then it was coated with a thin layer of gold by a coating instrument (Leica EM ACE600).

Glyphosate adsorption

The synthetic zeolite NaY and Fe loaded zeolite NaY were used as adsorbents for glyphosate adsorption. Their adsorption kinetic behavior was studied through a batch process at various times. Firstly, the adsorbent (0.05 g) was added to a 50 mg/L glyphosate aqueous solution (20 mL). The solution pH was adjusted to 4 by 0.1 M NaOH and 0.1 M HCl. The adsorption was monitored at 30 $\pm$ 1 °C under stirring with a speed of 300 rpm. The adsorption mixture was withdrawn by a syringe at the adsorption times of 15, 30, 60, 120, 150 and 180 min. The adsorbents were removed from the mixture by filtration using a nylon filter with a pore size of 0.45 μm. Glyphosate concentration was determined by a colorimetric method using UV-Visible spectrometer (T80+, PG instruments limited). The adsorption capacity of the adsorbents can be calculated from an Eq. (1);

$$AC = \frac{C_i - C_f}{W} \times V \quad (1)$$

The AC (mg/g) is adsorption capacity. C_i (mg/L) and C_f (mg/L) are the concentration of glyphosate before and after adsorption experiments, respectively. W is the amount of adsorbent (g). V is the volume of glyphosate solution (L). For the adsorption isotherm study, the experiment was also performed as a

similar procedure to the adsorption kinetic study. The initial concentration of glyphosate aqueous solution was varying 40 to 350 mg/L.

Glyphosate analysis

Glyphosate concentration was measured by a colorimetric method according to the procedure from the work of Angélica *et al.* [24]. A calibration curve was prepared in the concentration range of 2 - 16 mg/L by a 500 mg/L stock solution. The stock solutions ranging from 20 - 160 μL were added to a series of test tubes. The 5 %w/v ninhydrin solution (1 mL) and 5 %w/v sodium molybdate solution (1 mL) were consecutively added to the test tubes, which were sealed and kept in a water bath at 90 °C for 12 min. The violet complex was appeared indicating the glyphosate foundation. After that the solution was cooled and adjusted the volume to 5 mL by DI water. The visible light absorption of the appearance violet complex was monitored at wavelength 570 nm by UV-Visible spectrometer (T80+, PG instruments limited). The blank and sample were also prepared in the same sense as the calibration curve, excluding the addition of glyphosate stock solution. Glyphosate concentration was plotted against absorbances to create the calibration curve.

Results and discussion

Characterizations results

Figure 1(a) shows XRD patterns of the synthetic zeolite NaY from the bagasse ash. The diffraction peaks were observed at 6.19, 10.17, 12.00, 15.67, 19.96, 23.53, 26.90 and 31.17 °, which refers to the FAU framework type of pure zeolite NaY (JCPDS 01-081-2466) [25]. The zeolite NaY had a Si/Al mass ratio of 2.29. Then it was further impregnated by Fe (1.75 - 7.66 %wt) according to the elemental analysis results presented in **Table 1**. The FAU framework of NaY still remained after Fe loading up to 7.66 %wt. The reduction in XRD diffraction intensity of the Fe-loaded NaY could be described by the coverage of Fe oxides on the zeolite surface [26]. However, the XRD peaks of Fe oxides were not observed because of low Fe loading. It was also found from the zeolite NaY with Fe loading < 9 %wt in the work of Yang *et al.* [21]. The surface area and pore volume of materials were analyzed by N_2 adsorption-desorption techniques. The N_2 adsorption-desorption isotherms of zeolite NaY and the Fe-loaded zeolite NaY are shown in **Figure 1(b)**. All samples exhibited type I, a microporous material according to the IUPAC classification [27]. The hysteresis loops starting at $p/p_0 \approx 0.45$ were observed to indicate the mesopore for all samples. It was from the particle aggregation leading to the interparticle voids [28]. The surface area (S_{BET}) and pore volume of samples are summarized in **Table 1**. The Fe-loaded zeolite NaY had lower S_{BET} and pore volume values as compared to the bare zeolite NaY. A drastic decrease in micropore volume was observed for all Fe-loaded zeolite NaY. It demonstrated that the iron filled the zeolite pore and dispersed on the zeolite surface. For the point of zero charge (pH_{pzc}), it was determined by the pH drift method to evaluate the possible attraction and repulsion between glyphosate and the synthetic adsorbents. At the solution pH values higher than pH_{pzc}, the adsorbent surface indicates a negative charge. On the other hand, at the solution pH values lower than pH_{pzc} value, the adsorbent surface indicates a positive charge [29]. In this work, the pH of glyphosate solution was adjusted to 4. Therefore, the surface charge of all adsorbents was positive. The decreasing of pHpzc value was observed and related to the increase of Fe contents. The similar result was observed from the work of Pereira *et al.* [29], the decreasing of ferrihydrite's pHpzc value was obtained after anion loaded onto the positive sites of the material. Therefore, the magnification of the positively charged surface of material could be estimated from the pHpzc. In addition, the zeta potentials (ζ) of adsorbents were measured in the solution at pH 4. They were negative values that arose from the signals of liquid ions of an opposite charge to the adsorbent's particles at a slipping plane. A higher negative value of ζ means a larger positively charged particle. As the results, the zeta potentials were corresponded to the pHpzc values of the adsorbents. It could be concluded that the zeolite NaY was a higher positively charged particle than the 1.75, 5.11 and 7.66 %Fe/NaY, respectively. **Figure 2** shows the SEM images of the zeolite NaY and the Fe-loaded zeolite NaY. The regular and uniform particles was observed and attributed to the zeolite NaY. For the Fe-loaded zeolite NaY, the particles with un-smoothed surface could obtain after the impregnation with Fe. This phenomenon also observed from the work of Krisnandi *et al.* [30].

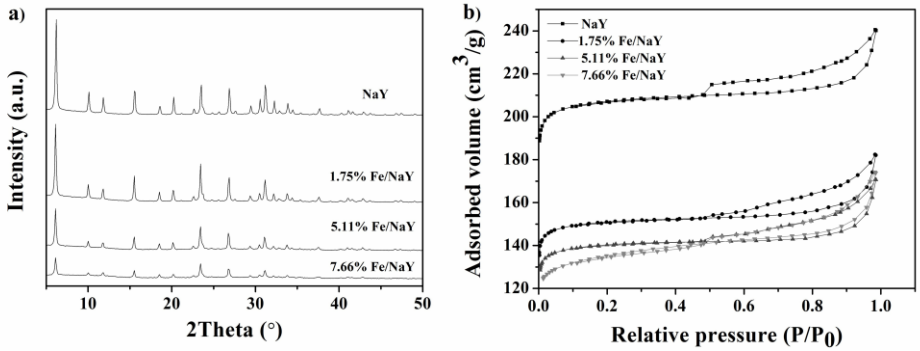


Figure 1 Powdered XRD patterns (a) and N_2 adsorption-desorption isotherms (b) of adsorbents.

Table 1 Physical properties and elemental contents of adsorbents.

Properties	Si/Al[a]	S_{BET}[b] (m^2/g)	Pore volume (cm^3/g)			pH_{pzc}[f]	ζ [g]
			Vtotal[c]	Vmicro[d]	Vmeso[e]		
NaY	2.29	627	0.319	0.306	0.066	7.50	−31.63
[a]1.75 %Fe/NaY	2.16	456	0.230	0.219	0.059	7.40	−26.37
[a]5.11 %Fe/NaY	2.07	423	0.216	0.203	0.056	6.85	−18.80
[a]7.66 %Fe/NaY	1.99	415	0.207	0.193	0.072	6.25	−18.60

[a]Elemental analysis by the ED-XRF technique.
[b]Total surface area (S_{BET}) by the BET method.
[c]Total pore volume by the Horvath-Kawazoe method at P/P0 = 0.97.
[d]Micropore volume by the *t*-plot method.
[e]Mesopore volume by the BJH method.
[f]Point of zero charges (pH_{pzc}) by the pH drift method.
[g]Zeta potential (ζ) by the Lazer Doppler electrophoresis technique.

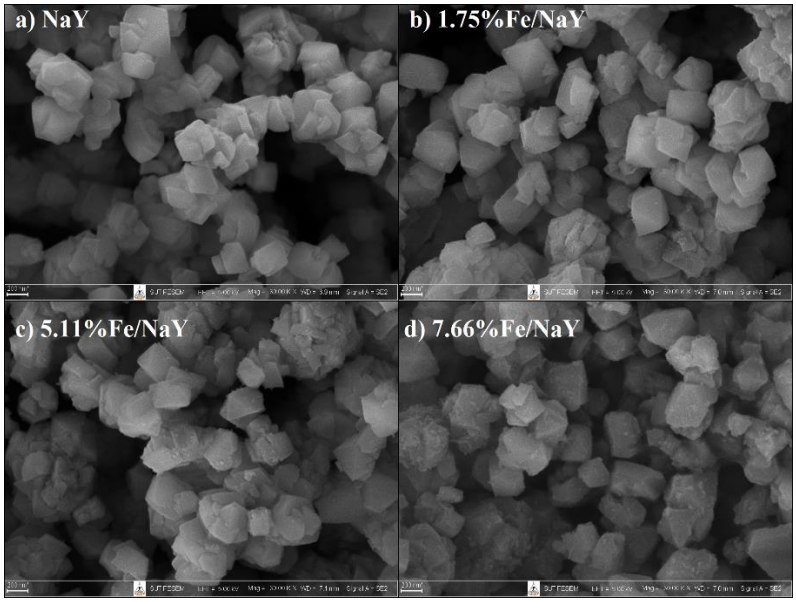


Figure 2 Scanning electron microscopy images of adsorbents (200 nm scale bar and 30 k magnification).

Adsorption kinetic results

The adsorption kinetics of zeolite NaY and Fe-loaded zeolite NaY were studied by using the initial glyphosate concentration of 50 mg/L at pH of 4. The results are shown in **Figure 3**. The adsorption was fast at the beginning and then reached equilibrium at 180 min. From the pKa values of the glyphosate which consist of 0.78, 2.29, 5.96 and 10.90, [31] the glyphosate could be deprotonated at pH of 4 and give 1 negative net charge arising from the 2 negative charges of the phosphonic and carboxylate ends and 1 positive charge of the amino group [32]. On the other hand, the silanol group (Si-OH) of zeolite NaY was protonated as $Si\text{-}OH_2^+$ which indicates the positively charged surface according to the pH_{pzc} result. The electrostatic interaction [33,34] and the hydrogen bond [35] were responsible for glyphosate adsorption. Although the zeolite NaY was the most positively charged adsorbent with the greatest surface area and porosity in this study, it had the lowest adsorption capacity. Because zeolite NaY had a high hydrophilicity, competitive water adsorption could occur, suppressing glyphosate adsorption [36]. For the Fe-loaded zeolite NaY, their glyphosate adsorption capacity was higher than the bare zeolite NaY. The Fe could coordinate with the glyphosate's phosphonic end forming a complexation which was monitored by ATR-FTIR [9].

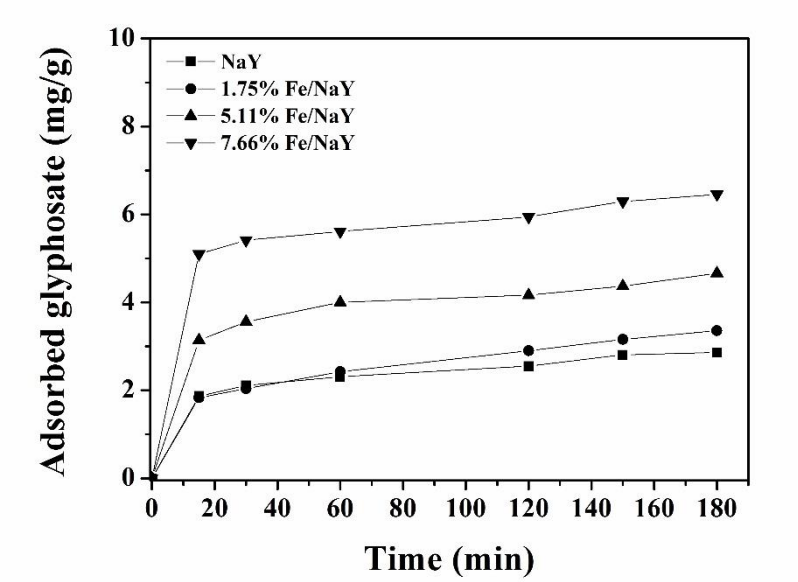


Figure 3 Adsorption of glyphosate by the adsorbents at various times (initial glyphosate concentration of 50 mg/L; the ratio of adsorbent/glyphosate solution of 0.05g/20 mL; stirring speed of 300 rpm at pH of 4).

To clarify the kinetic behavior of all adsorbents, the pseudo-first order model (PFO), pseudo-second order model (PSO) and Elovich model (ELV) were used to analyze all adsorption data. The linear equations of PFO and PSO are represented by the Eqs. (2) and (3), respectively. The PFO is the plot of log (q_e - q_t) versus t meanwhile, the PSO is the plot of t/q_t versus t. The initial glyphosate adsorption rate (h) can be evaluated from the reciprocal of the intercept according to the Eq. (4);

$$\log(q_e - q_t) = \log q_e - \frac{k_1 t}{2.303} \quad (2)$$

$$\frac{t}{q_t} = \frac{1}{k_2 q_e^2} + \frac{t}{q_e} \quad (3)$$

$$h = k_2 q_e^2 \quad (4)$$

The q_e and q_t are amount of glyphosate adsorbed onto the adsorbents (mg/g) at equilibrium and at time t, respectively. k_1 and k_2 are rate constant for the pseudo-first order model (min^{-1}) and the pseudo-second order model ($g.mg^{-1}.min^{-1}$). The faster adsorption is the higher rate constant value [37]. Moreover, the ELV model is also used to describe the chemisorption on heterogeneous adsorbents. The linear equation

is as Eq. (5) Where α is the initial glyphosate adsorption rate ($mg.g^{-1}.min^{-1}$) and β is the adsorption constant ($g.mg^{-1}$). They can be evaluated from the plot of q_t versus ln t.

$$q_t = \frac{\ln(\alpha\beta)}{\beta} + \frac{\ln t}{\beta} \quad (5)$$

Figure 4 shows the linear variation for the PFO (a) PSO (b) and ELV (c) models of the prepared adsorbents. The adsorption kinetic parameters were summarized in **Table 2**. The correlation coefficient R^2 close to 1 and a smaller difference in glyphosate adsorption capacity between the calculation and the experiment were used to assess the reliability of the kinetic data. As the results, all adsorbents best explained by the PSO model rather than the other models. It suggested that the rate determining step was controlled by chemisorption. The fastest adsorption was observed by using the zeolite NaY as an adsorbent. It provided the highest rate constant (k_2) of 2.38×10^{-2} $g.mg^{-1}.min^{-1}$ which is probably due to its highest surface area and porosity. In case of the Fe loaded zeolite NaY, the k_2 and h increased with the Fe content. By the maximum adsorption capacities were 6.46, 4.66, 3.36 and 2.86 mg/g for 7.66, 5.11, 1.75 %Fe/NaY and NaY, respectively. Therefore, the interaction between glyphosate and Fe was the key-driven force for this adsorption.

Furthermore, the cause of adsorption was studied by the intra-particle diffusion model (IPD). The linear equation is represented by an Eq. (6), which is the plot of q_t versus $t^{1/2}$ as represented in **Figure 4(d)**. The K_{IPD} is the intra-particle diffusion constant ($mg.g^{-1}.min^{1/2}$) and C is the thickness of boundary layer (intercept).

$$q_t = K_{IPD}t^{1/2} + C \quad (6)$$

The kinetic parameters for IPD model were also summarized in **Table 2**. The correlation coefficient R^2 is greater than 0.95 for the adsorbents. All linear plots did not pass through the origin (**Figure 3(d)**), indicating that intra-particle diffusion is not the only rate-determining step in adsorption [38]. External diffusion may have had an impact on the process [39]. The larger C value was observed by the adsorbents with a higher Fe loading. It used to define the distance from the adsorbent where the adsorbate concentration reaches 99 % of the bulk concentration. With a larger C value, higher adsorption capacity is achieved [40].

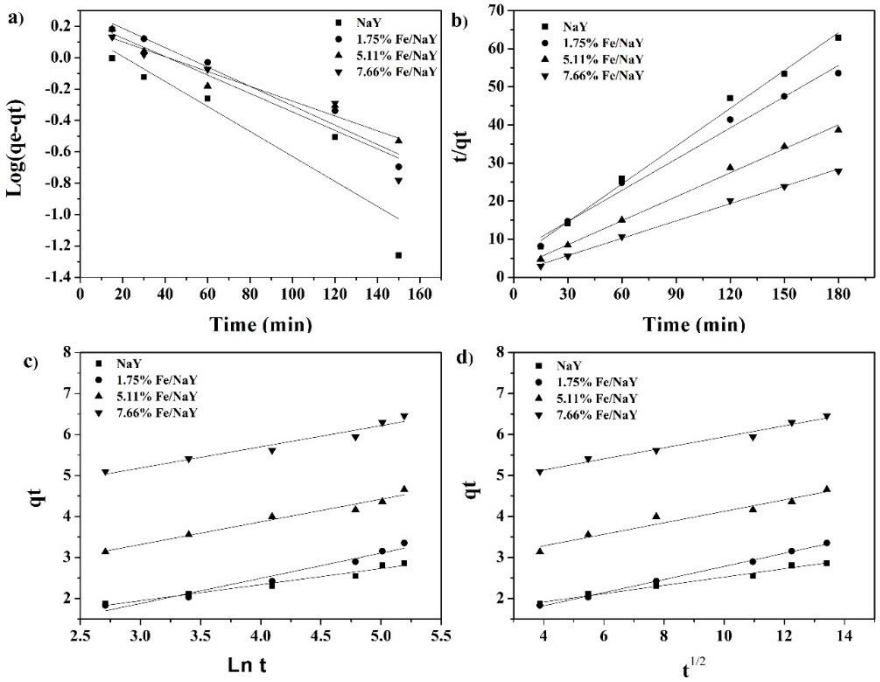


Figure 4 Linear plots of (a) pseudo-first order model (PFO), (b) pseudo-second order model (PSO), (c) Elovich model (ELV) and (d) intra-particle diffusion model (IPD) for the adsorbents.

Table 2 Adsorption kinetic parameters of glyphosate onto adsorbents.

Kinetic models	Parameters	Adsorbents			
		NaY	**1.75 %Fe/NaY**	**5.11 %Fe/NaY**	**7.66 %Fe/NaY**
PFO	q_{exp}	2.86	3.36	4.66	6.46
	q_{cal}	1.47	1.99	1.57	1.75
	K_1	1.80×10^{-2}	1.20×10^{-2}	1.10×10^{-2}	1.40×10^{-2}
	R^2	0.8581	0.7832	0.9473	0.8954
PSO	q_{exp}	2.86	3.36	4.66	6.46
	q_{cal}	2.80	3.28	4.50	6.33
	K_2	2.38×10^{-2}	1.17×10^{-2}	1.96×10^{-2}	2.02×10^{-2}
	h	0.22	0.16	0.44	0.88
	R^2	0.9942	0.9894	0.9954	0.9972
ELV	α	2.81	0.76	11.13	5.89×10^{2}
	β	2.55	1.63	1.81	1.94
	R^2	0.9696	0.9643	0.9691	0.9455
IPD	K_{IPD}	0.1013	0.1602	0.1403	0.1346
	C	1.5125	1.1839	2.5257	4.5993
	R^2	0.9853	0.9980	0.9511	0.9792

PFO is pseudo-first order model.
PSO is pseudo-second order model.
ELV is Elovich model.
IPD is intra-particle diffusion model.

Adsorption isotherm results

The interactions between glyphosate and adsorbents were investigated further for the purpose of predicting water treatment conditions through the adsorption isotherms. The experiment was performed at 30 °C by varying the initial concentrations of glyphosate (35 - 375 mg/L). The adsorption data were analyzed by Langmuir and Freundlich adsorption isotherm models. The Langmuir model is valid for monolayer adsorption onto the adsorbent with a homogeneous surface. Conversely, the Freundlich model is valid for multilayer adsorption onto the adsorbent with a heterogeneous surface. The linear equations of Langmuir and Freundlich adsorption isotherm models are presented by the Eqs. (7) and (8);

$$\frac{1}{q_e} = \frac{1}{q_m K_L C_e} + \frac{1}{q_m} \quad (7)$$

$$\log q_e = \frac{1}{n}\log C_e + \log K_F \quad (8)$$

Where Ce is the glyphosate concentration at equilibrium (mg/L). qm is the maximum monolayer adsorption capacity of adsorbent (mg/g) and K_L is a Langmuir constant (L/mg). K_F is a Freundlich isotherm constant that indicating the relative adsorption capacity of adsorbent (mg/g) and n is adsorption intensity. The accuracy of the adsorption isotherm can be verified by Chi-square values ($\chi 2$) which is calculated from the Eq. (9) where $q_{e,e}$ and $q_{e,m}$ are amount of glyphosate adsorbed on adsorbent (mg/g) at equilibrium derived from the experiment and the calculation, respectively.

$$\chi 2 = \frac{\sum(q_{e,e} - q_{e,m})^2}{q_{e,m}} \quad (9)$$

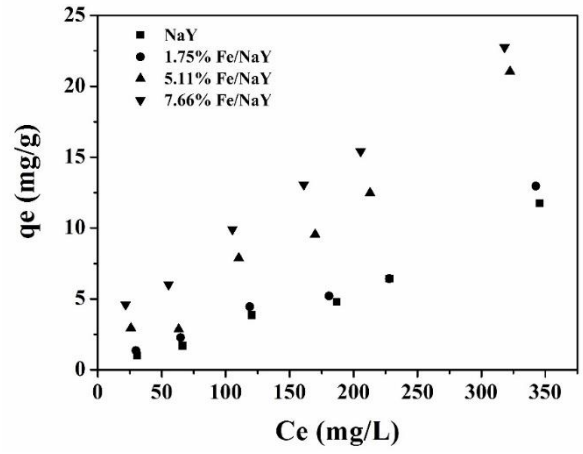


Figure 5 Adsorption isotherms of glyphosate by the adsorbents.

Figure 5 shows the adsorption isotherms of glyphosate at equilibrium time (180 min). The Langmuir isotherm and Fruendlich isotherm models were used to fit the adsorption isotherm data as shown in **Figure 6**. The obtained isotherm parameters were summarized into **Table 3**. The fitting degree of isotherm models for the experimental data was analyzed by the correlation coefficient R^2 value close to 1 together with a small value of $\chi 2$. As the results, all adsorbents best explained by Fruendlich isotherm model with the R^2 values more than 0.98 and $\chi 2$ values of 0.08 - 0.70. Therefore, the glyphosate was multilayer adsorbed onto the prepared adsorbents, which containing energetic surface heterogeneity [41]. The K_F values referred to the adsorption capacity of adsorbents which the Fe-loaded zeolite NaY provided a higher K_F values than zeolite NaY. They were following as 0.7494, 0.2177, 0.0956 and 0.0280 mg/g for 7.66, 5.11, 1.75 %Fe/NaY and NaY, respectively. In general, the 1/n value is used to indicate the heterogeneity of the adsorption surface and the adsorbate-adsorbent interaction. If 1/n value is less than 1, it indicates a favorable adsorption. A smaller 1/n value also indicates a larger adsorption surface heterogeneity [42] and a stronger adsorbate-adsorbent interaction. [43] In addition, the cooperative adsorption occurs when the 1/n value is higher than 1 [43,44]. From the 1/n values (**Table 3**), they were 0.5728, 0.7698, 0.7775 and 1.0169 for 7.66, 5.11, 1.75 %Fe/NaY and NaY, respectively. The Fe-loaded zeolite NaY exhibited the 1/n values < 1, which indicating a strong glyphosate-adsorbent interaction. Using an adsorbent with a higher Fe loading could result in a stronger interaction. This suggested that loading of Fe onto zeolite NaY provided heterogeneous surfaces with a high affinity for glyphosate molecules.

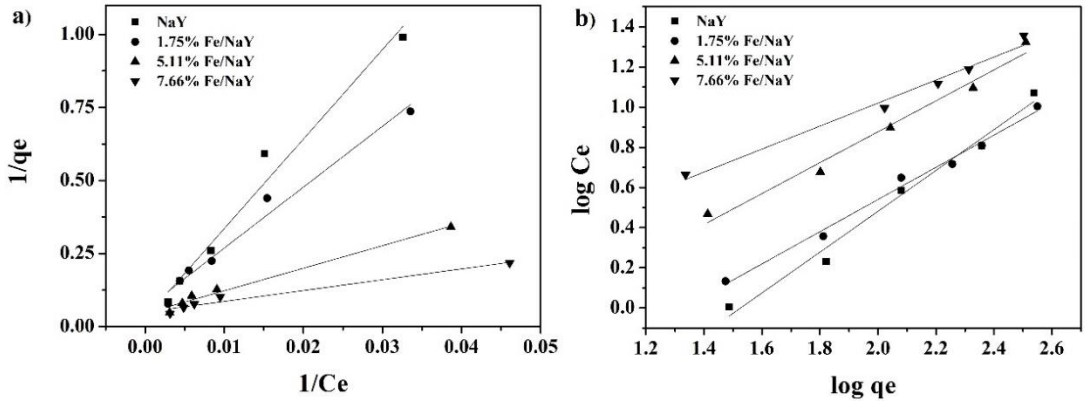


Figure 6 (a) Langmuir and (b) Freundlich plots for the adsorption of glyphosate by the adsorbents.

Table 3 Langmuir and freundlich isotherm parameters for the adsorption of glyphosate by the adsorbents.

Adsorbents	Langmuir isotherm				Freundlich isotherm			
	Q_m (mg/g)	K_L (L/mg)	χ^2	R^2	K_F	1/n	χ^2	R^2
NaY	47.8469	0.0007	0.8351	0.9766	0.0280	1.0169	0.2189	0.9850
1.75 %Fe/NaY	16.6113	0.0029	2.7849	0.9793	0.0956	0.7775	0.0928	0.9873
5.11 %Fe/NaY	22.1729	0.0058	3.2528	0.9849	0.2177	0.7698	0.0815	0.9879
7.66 %Fe/NaY	20.4499	0.0132	2.7549	0.9683	0.7494	0.5728	0.7042	0.9810

Conclusions

The zeolite NaY was successfully synthesized from bagasse ash and being loaded with 1.75 - 7.66 %wt of Fe by impregnation method. They were used as adsorbent for glyphosate adsorption. The decrease of S_{BET} and pore volume of the materials was observed after Fe loading indicating that the Fe was located inside the zeolite pore and on the zeolite surface. The effect of the adsorbents with varying Fe contents on the glyphosate adsorption was studied in a batch process at pH 4. At this point, the glyphosate molecule was deprotonated giving a negatively charged molecule which could be adsorbed on the positively charged surface of the prepared adsorbents. The presence of Fe decreased the material's pH_{pzc} and zeta potential values resulting in a less positively charged adsorbent. Although the zeolite NaY had the highest values of surface area, porosity, and positive charge magnification, its adsorption capacity was the lowest as compared to the Fe loaded zeolite NaY. Therefore, the complexation between the Fe and glyphosate anion played an important role for the adsorption rather than the electrostatic attraction. For all adsorbents, the pseudo-second order model was the best fitted with the experimental data ($R^2 > 0.98$). The rate determining step was controlled by a chemisorption. The adsorption rate constants (K_2) were 2.38×10^{-2}, 2.02×10^{-2}, 1.96×10^{-2} and 1.17×10^{-2} $g.g^{-1}.min^{-1}$ for NaY, 7.66, 5.11, 1.75 %Fe/NaY, respectively. The faster adsorption was observed over the adsorbent with a higher Fe content. The intra-particle diffusion model was also well fitted with the experimental data ($R^2 > 0.95$). The linear plots did not pass through the origin indicating that both external diffusion and intra-particle diffusion involved the rate determining step. At the adsorption equilibrium, all adsorbents were best described by the Fruendlich adsorption isotherm model ($R^2 > 0.98$). The adsorption capacity (K_F) were 0.7494, 0.2177, 0.0956 and 0.0280 mg/g for 7.66, 5.11, 1.75 %Fe/NaY and NaY, respectively. Therefore, the glyphosate was multilayer adsorbed onto the prepared adsorbents, which containing energetic surface heterogeneity. A larger energetic surface heterogeneity and stronger adsorbate-adsorbent interaction were obtained from the adsorbent with a higher Fe content.

Acknowledgements

This work was financially supported by Burapha University and Thailand Science Research and Innovation (TSRI) (Grant no. 30/2565).

References

[1] Ministry of Agriculture and Cooperative. Thailand foreign agricultural trade statistics (*in Thai*), Available at: https://www.oae.go.th/assets/portals/1/ebookcategory/43_trade2564/, accessed October 2022.

[2] Ministry of Agriculture and Cooperative. Summary of Imported Pesticides into Thailand (*in Thai*), Available at: https://www.doa.go.th/ard/?page_id=386, accessed October 2022.

[3] AK Mishra, DN Tiwari and AN Rai. *Cyanobacteria: From basic science to applications*. Academic Press London, London, 2019.

[4] D Noicharoen, P Parkpian, O Shipin, C Polprasert, R DeLaune and M Kongchum. Effect of salinity on adsorption and desorption of paraquat in Pak Phanang river sediment, Thailand. *J. Environ. Sci. Health A* 2012; **47**, 1897-908.

[5] R Anlauf, J Schaefer and P Kajitvichyanukul. Coupling HYDRUS-1D with ArcGIS to estimate pesticide accumulation and leaching risk on a regional basis. *J. Environ. Manag.* 2018; **217**, 980-90.

[6] Some Organophosphate Insecticides and Herbicides. IARC Monographs on the Evaluation of Carcinogenic Risks to Humans Volume 112, Available at: https://publications.iarc.fr/549, accessed October 2022.

[7] A Serra-Clusellas, LD Angelis, M Beltramo, M Bava, JD Frankenberg, J Vigliarolo, ND Giovanni, JD Stripeikis, JA Rengifo-Herrera and MMFD Cortalezzi. Glyphosate and AMPA removal from water by solar induced processes using low Fe(III) or Fe(II) concentrations. *Environ. Sci. Water Res. Tech.* 2019; **5**, 1932-42.

[8] HA Pereira, PRT Hernandes, MS Netto, GD Reske, V Viecell, LTS Oliveria and GL Dotto. Adsorbents for glyphosate removal in contaminated waters: A review. *Environ. Chem. Lett.* 2021; **19**, 1525-43.

[9] BC Barja and MDS Afonso. An ATR-FTIR study of glyphosate and its Fe(III) complex in aqueous solution. *Environ. Sci. Tech.* 1998; **32**, 3331-5.

[10] J Sheals, S Sjöberg and P Persson. Adsorption of glyphosate on goethite: molecular characterization of surface complexes. *Environ. Sci. Tech.* 2018; **36**, 3090-5.

[11] S Kaur, V Kumar, M Chawla, L Cavallo, A Poater and N Upadhyay. Pesticides curbing soil fertility: Effect of complexation of free metal ions. *Front. Chem.* 2017; **4**, 43.

[12] D Jia, M Liu, J Xia and C Li. Effective removal of aqueous glyphosate using $CuFe_2O_4$@biochar derived from phragmites. *J. Chem. Tech. Biotechnol.* 2019; **95**, 196-204.

[13] Y Li, C Zhao, Y Wen, Y Wang and Y Yang. Adsorption performance and mechanism of magnetic reduced graphene oxide in glyphosate contaminated water. *Environ. Sci. Pollut. Res.* 2018; **25**, 21036-48

[14] Z Ren, Y Dong and Y Liu. Enhanced glyphosate removal by montmorillonite in the presence of Fe(III). *Ind. Eng. Chem. Res.* 2014; **53**, 14485-92.

[15] G Xiao and Q Meng. D151 resin preloaded with Fe^{3+} as a salt resistant adsorbent for glyphosate from water in the presence 16 % NaCl. *Ecotoxicol. Environ. Saf.* 2020; **190**, 110140.

[16] R Liu, Y Xie, K Cui, J Xie, Y Zhang and Y Huang. Adsorption behavior and adsorption mechanism of glyphosate in water by amino-MIL-101(Fe). *J. Phys. Chem. Solid.* 2022; **161**, 110403.

[17] M Milojević-Rakić, A Janošević, J Krstić, BN Vasiljević, V Dondur and G Ćirić-Marjanović. Polyaniline and its composites with zeolite ZSM-5 for efficient removal of glyphosate from aqueous solution. *Microporous Mesoporous Mater.* 2013; **180**, 141-55.

[18] D Janićijević, A Jevremović, A Janošević Ležaić, B Nedić Vasiljević, S Uskoković-Marković, D Bajuk-Bogdanović and M Milojević-Rakić. Comparative assessment of pesticide adsorption capacity and antioxidant activity of Silver dodecatungstophosphate/HBEA zeolite composites. *J. Environ. Chem. Eng.* 2021; **9**, 106341.

[19] S Zavareh, Z Farrokhzad and F Darvishi. Modification of zeolite 4A for use as an adsorbent for glyphosate and as an antibacterial agent for water. *Ecotoxicol. Environ. Saf.* 2018; **155**, 1-8.

[20] FM Flores, RMT Sánchez and MDS Afonso. Some aspects of the adsorption of glyphosate and its degradation products on montmorillonite. *Environ. Sci. Pollut. Res.* 2018; **25**, 18138-46.

[21] X Yang, X Cheng, AA Elzatahry, J Chen, A Alghamdi and Y Deng. Recyclable fenton-like catalyst based on zeolite Y supported ultrafine, highly-dispersed Fe_2O_3 nanoparticles for removal of organics under mild conditions. *Chin. Chem. Lett.* 2019; **30**, 324-30.

[22] P Chindaprasirt and U Rattanasak. Eco-production of silica from sugarcane bagasse ash for use as a photochromic pigment filler. *Sci. Rep.* 2020; **10**, 9890.

[23] K Rintramee, L Sujarit and S Kornsanthia. Fe_2O_3 on zeolite NaY synthesized from rice husk as catalyst for oxidation of styrene. *RMUTP Res. J.* 2019; **13**, 1-11.

[24] ÁBM Angélica, MC Aymer, RJG Amaya and MA Amner. Occurrence of glyphosate in surface and drinking water sources in Cúcuta, Norte de Santander, and its removal using membrane technology. *Front. Environ. Sci.* 2022; **10**, 941836.

[25] MMJ Treacy and JB Higgins. *Collection of simulated XRD powder patterns for zeolites*. Elsevier Science, Amsterdam, Netherlands, 2007.

[26] NA Jamalluddin and AZ Abdullah. Low frequency sonocatalytic degradation of Azo dye in water using Fe-doped zeolite Y catalyst. *Ultrason. Sonochem.* 2014; **21**, 743-53.

[27] J Rouquerol, D Avnir, CW Fairbridge, DH Everett, JM Haynes, N Pernicone, JDF Ramsay, KSW Sing and KK Unger. Recommendations for the characterization of porous solids (technical report). *Pure Appl. Chem.* 1994; **66**, 1739-58.

[28] L Mu, WW Feng, H Zhang, X Hu and Q Cui. Synthesis and catalytic performance of a small crystal NaY zeolite with high SiO_2/Al_2O_3 ratio. *RSC Adv.* 2019; **9**, 20528-35.

[29] RC Pereira, PR Anizelli, ED Mauro, DF Valezi, ACSD Costa, CTBV Zaia and DAM Zaia. The effect of pH and ionic strength on the adsorption of glyphosate onto ferrihydrite. *Geochem. Trans.* 2019; **20**, 3.

[30] YK Krisnandi, DA Nurani, DV Alfian, U Sofyani, M Faisal, IR Saragi, AZ Pamungkas and AP Pratama. The new challenge of partial oxidation of methane over Fe_2O_3/NaY and Fe_3O_4/NaY heterogeneous catalysts. *Heliyon* 2021; **7**, e08305.
[31] L Rivoira, M Appendini, S Fiorilli, B Onida, MD Bubba and MC Bruzzoniti. Functionalized iron oxide/SBA-15 sorbent: investigation of adsorption performance towards glyphosate herbicide. *Environ. Sci. Pollut. Res.* 2016; **23**, 21682-91.
[32] LL Borba, RMF Cuba, FJC Terán, MN Castro and TA Mendes. Use of adsorbent biochar from Pequi (*Caryocar brasiliense*) husks for the removal of commercial formulation of glyphosate from aqueous media. *Braz. Arch. Biol. Tech.* 2019; **62**, e19180450.
[33] H Qu, S Bhattacharyya and P Ducheyne. Sol-gel processed oxide controlled release materials. *Compr. Biomater.* 2017; **4**, 475-95.
[34] I Herath, P Kumarathilaka, MI Al-Wabel, A Abduljabbar, M Ahmad, ARA Usman and M Vithanage. Mechanistic modeling of glyphosate interaction with rice husk derived engineered biochar. *Microporous Mesoporous Mater.* 2016; **225**, 280-8.
[35] PJ Espinoza-Montero, C Vega-Verduga, P Alulema-Pullupaxi, L Fernández and JL Paz. Technologies employed in the treatment of water contaminated with glyphosate: A review. *Molecules* 2020; **25**, 5550.
[36] J Chen, LL Gao, Q Jiang, Q Hou, Y Hong, WJ Shen, Y Wang and JH Zhu. Fabricating efficient porous sorbents to capture organophosphorus pesticide in solution. *Microporous Mesoporous Mater.* 2020; **294**, 109911.
[37] QC Liu, YR Zhou, M Wang, Q Zhang, T Ji, TY Chen and DC Yu. Adsorption of methylene blue from aqueous solution onto viscose-based activated carbon fiber felts: Kinetics and equilibrium studies. *Adsorption Sci. Tech.* 2019; **37**, 312-32.
[38] TR Sahoo and B Prelot. *Adsorption processes for the removal of contaminants from wastewater: the perspective role of nanomaterials and nanotechnology*. *In*: B Bonelli, FS Freyria, I Rossetti and R Sethi (Eds.). Nanomaterials for the Detection and Removal of Wastewater Pollutants. Elsevier, Amsterdam, Netherlands, 2020.
[39] S Yadav and N Singh. Sugarcane trash ash: A low cost adsorbent for atrazine and fipronil removal from water. *Indian J. Chem. Tech.* 2020; **27**, 319-25.
[40] A Pholosi, EB Naidoo and AE Ofomaja. Intraparticle diffusion of Cr(VI) through biomass and magnetite coated biomass: A comparative kinetic and diffusion study. *S. Afr. J. Chem. Eng.* 2020; **32**, 39-55.
[41] X Chen. Modeling of experimental adsorption isotherm data. *Information* 2015; **6**, 14-22.
[42] UA Edet and AO Ifelebuegu. Kinetics, isotherms, and thermodynamic modeling of the adsorption of phosphates from model wastewater using recycled brick waste. *Processes* 2020; **8**, 665.
[43] VO Shikuku and T Mishra. Adsorption isotherm modeling for methylene blue removal onto magnetic kaolinite clay: A comparison of two-parameter isotherms. *Appl. Water Sci.* 2021; **11**, 103.
[44] ABD Nandiyanto, SN Hofifah, S Anggraeni and T Kurniwan. Isotherm adsorption of 40-μm zeolite particles for treatment of dye wastewater. *J. Eng. Sci. Tech.* 2022; **17**, 1265-75.